

Article

Obtention of a Sensitive Acylated Pyrogallol[4]arene-Based Sensor for the Detection of Carnitine: A Spectroscopic and DRX Study

José Luis Casas-Hinestroza ¹, Adrián Pérez-Redondo ² and Mauricio Maldonado ^{1,*}

¹ Departamento de Química, Facultad de Ciencias, Sede Bogotá, Universidad Nacional de Colombia, Carrera 30 No. 45-03, Bogotá 111231, Colombia; jlcasash@unal.edu.co

² Departamento de Química Orgánica y Química Inorgánica, Instituto de Investigación Química “Andrés M. del Río” (IQAR), Universidad de Alcalá, 28805 Alcalá de Henares, Madrid, Spain; adrian.perez@uah.es

* Correspondence: mmaldonadov@unal.edu.co

Abstract: Complexation between carnitine and acetylated or benzylated pyrogallol[4]arenes was studied in DMSO via dynamic NMR, UV-vis spectroscopy, and in the gas phase via electrospray ionization-mass spectrometry (ESI-MS). In the presence of benzylated tetra(phenyl)pyrogallol[4]arene, the interaction with carnitine via NMR was evident and was confirmed by means of UV-vis spectroscopy, where the formation of a host–guest-type complex was observed; this was stable and exhibited a change to a clear color. With benzylated tetra(propyl)pyrogallol[4]arene, the results showed that there was no interaction with the neurotransmitter. A plausible explanation for this behavior is based on the dynamic behavior of the benzylated tetra(propyl)pyrogallol[4]arene, and this shows the dependence on the size of the cavities and the substituent on the lower rim of the pyrogallo[4]arenes. Suitable crystals of *O*-acetylated-tetra(propyl)calix[4]pyrogallolarene were obtained and were characterized through an X-ray crystal structure determination.

Keywords: *crown* conformer; benzylated pyrogallol[4]arene; host-guest complex; neurotransmitters



Citation: Casas-Hinestroza, J.L.; Pérez-Redondo, A.; Maldonado, M. Obtention of a Sensitive Acylated Pyrogallol[4]arene-Based Sensor for the Detection of Carnitine: A Spectroscopic and DRX Study. *Analytica* **2024**, *5*, 576–586. <https://doi.org/10.3390/analytica5040038>

Academic Editor: Marcello Locatelli

Received: 3 September 2024

Revised: 25 October 2024

Accepted: 31 October 2024

Published: 14 November 2024



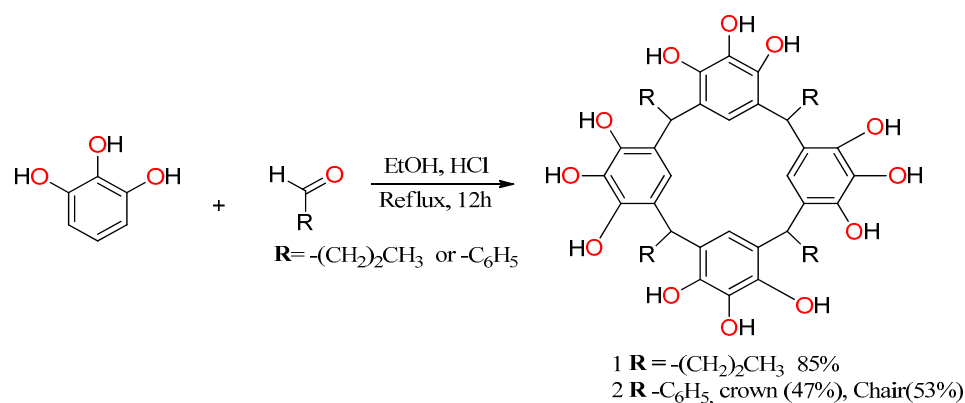
Copyright: © 2024 by the authors. Licensee MDPI, Basel, Switzerland. This article is an open access article distributed under the terms and conditions of the Creative Commons Attribution (CC BY) license (<https://creativecommons.org/licenses/by/4.0/>).

1. Introduction

Currently, there are many substances in nature that have attracted the attention of researchers due to their activity in biological systems. An interesting group of substances are neurotransmitters, which play a crucial role in the proper functioning of many biological processes. In this context, carnitine, a neurotransmitter derived from methionine and lysine, is a naturally occurring substance that is recognized as a nutritional supplement in the treatment of cardiovascular disease in the human body. A deficiency of L-carnitine leads to major energy loss and toxic accumulations of free fatty acids [1,2]. Many methods have been used to detect L-carnitine, such as spectrophotometric determination [3], HPLC-chromatography [4], mass spectrometry [5,6], capillary electrophoresis [7], NMR spectroscopy [8], and fluorescence [9], among others. However, there are still great challenges ahead for finding selective, sensitive tools for detecting carnitine. The study of the interactions of macrocycle systems with carnitine is key in many promising methods of detecting this neurotransmitter, as evidenced in recent publications [10,11]. In consideration of the above, polyhydroxylated platforms such as pyrogallol[4]arenes are compounds that have a wide range of applications in the detection of cations, anions, and neutral molecules [12–15].

The best synthetic route for producing Pyrogallo[4]arenes is the cyclocondensation reaction between pyrogallol and an aliphatic or aromatic aldehyde in acid media [16] (Scheme 1). These macrocyclic compounds may exist in various isomeric states: crown, chair, and boat. Of these isomers, the crown conformer (*rccc*) is the most thermodynamically stable compound. Alternatively, the conformation of pyrogallolarenes can be rigidified into

a crown by linking the hydroxyl groups of the upper rim, which provides a higher degree of preorganization [17]. In solution, the *rccc* isomer may adopt crown and boat conformations, which interconvert at room temperature. Studies of the conformational properties of pyrogallolarenes modified on the lower rim show that the most stable conformer in solution is the crown state, and this trend is favored by bulky substituents in the macrocyclic ring [18]. The functionalization of pyrogallol[4]arenes can be performed by varying the nature of the substituent group on the aldehyde, which facilitates the modification of the macrocyclic system on the lower rim. On the upper rim, the obvious site for chemical modification is the hydroxyl group, and it can be modified by acetylhydrazide [19], 2-bromo-isobutyryl bromide [20], alkylating reagents [21], sulfuric acid [22], and esterification [23], among others. These modifications can be used to form extended cavities, or it can be substituted by functional groups in specific applications.



Scheme 1. Synthesis of pyrogallol[4]arenes.

Continuing with our research on the reactivity and molecular interactions of polyhydroxylated platforms [24–27], in the present study, we show the reaction of C-tetra(propyl)pyrogallol[4]arene (1) and C-tetra(phenyl)pyrogallo[4]arene (2) (Scheme 1) with benzoyl chloride or acetic anhydride to generate polyacylated macrocycles.

The products were analyzed using ^1H - and ^{13}C -NMR, FTIR spectroscopy, and ESI-MS. UV-Vis spectroscopy was used to evaluate the interaction of the polybenzylated macrocycle with carnitine, and from the results, the important effect of the benzoyl group on the upper rim of the macrocycles was evident. Dynamic ^1H -NMR studies allowed us to understand the weak interaction of polybenzylated C-tetra(propyl) pyrogallo[4]arene with carnitine in DMSO.

2. Materials and Methods

Pyrogallol (CAS 87-66-1), ethanol (CAS 64-17-5), hydrochloric acid (CAS 7647-01-0), butyraldehyde (CAS 123-72-8), benzaldehyde (CAS 100-52-7), benzoyl chloride (CAS 98-88-4), chloroform (CAS 67-66-3), sodium hydroxyde (CAS 1310-73-2), sodium sulfate (7757-82-6), acetic anhydride (108-24-7), pyridine (110-86-1) and N,N-Diisopropylethylamine (CAS 108-24-7), which were required for the synthesis, were obtained from commercial sources and used as received without additional purification. Solvents were purified according to standard procedures.

The IR spectra were recorded on a Thermo-Fisher Scientific Nicolet iS10 FTIR spectrometer with a monolithic diamond ATR accessory and absorption in cm^{-1} (Thermo Scientific, Waltham, MA, USA). The ^1H - and ^{13}C -NMR spectra were recorded at 400 MHz on a Bruker Advance 400 instrument (Bruker, Billerica, MA, USA). Chemical shifts are reported in ppm, using the solvent residual signal. The molar mass was determined using an electrospray ionization Agilent 6470 triple quadrupole mass spectrometer (Santa Clara, CA, USA). Agilent Mass Hunter Workstation software (version B.09, Santa Clara, CA, USA)

was used for data acquisition and analysis. Melting points were measured on a Stuart apparatus (Cole-Parmer, Stafford, UK) and were not corrected.

Synthesis of pyrogallol[4]arenes

First, 5 mmol (0.660 g) of pyrogallol was dissolved in 20 mL of ethanol and cooled for one hour in a bath of ice. Then, 0.4 mL of hydrochloric acid (37%) and 0.5 mL (5 mmol) of aldehyde (butyraldehyde or benzaldehyde) were added dropwise to that solution. The reaction mixture was stirred and heated to 80 °C for 12 h, and the solid precipitate was filtered and washed with a water/ethanol (1:1) mixture, producing a pink and white solid with 60% yield, which was characterized using IR, ¹H-NMR, ¹³C-NMR, and ESI-MS. The separation of the boat and chair conformers of tetra(phenyl)pyrogallol[4]arene was carried out by using the technique described in the literature [23].

C-tetra(propyl)pyrogallol[4]arene (crown) (1) m.p. > 250 °C IR (ATR/cm⁻¹): 3413–3624 (broad), 2952, 2927, 2862, 2023, 1619, 1946, 1466, 1383, 1301, 1239, 1189, 1114, 1070, 1041, 982, 785, 612, 475, 418 cm⁻¹, ¹H-NMR (400 MHz, DMSO-*d*₆) δ 8.59 (b. s, 12H, OH); 6.92 (s, 4H, Ar-H); 4.17–4.21 (t, 4H, CH), 2.14–2.19 (m, 8H, CH₂); 1.18–1.27 (m, 8H, CH₂); 0.90–0.94 (t, *J* = 8 Hz, 12H, CH₃). ¹³C-NMR (400 MHz, DMSO-*d*₆) δ 139.6; 132.8; 124.5; 113.6; 34.9; 33.35; 20.7; 13.8. ESI-MS 743.4 [1 + Na]⁺.

C-tetra(phenyl)pyrogallol[4]arene (crown) (2) m.p. > 350 °C IR (ATR/cm⁻¹): 3300–3600 (broad), 1630, 1500, 1464, 1368, 1282, 1247, 1209, 1064, 1015, 163, 699, 566, 416 cm⁻¹; ¹H-NMR (400 MHz, DMSO-*d*₆): δ 7.77 (s, 4H, OH); 7.65 (s, 8H, OH); 6.95–6.96 (m, 12H, Ar); 6.76–6.77 (m, 8H, Ar); 6.04 (s, 4H, Ar); 5.78 (s, 4H, CH). ¹³C-NMR (100 MHz, DMSO-*d*₆): δ it (ppm) 145.4; 142.0; 131.8; 128.6; 127.0; 124.5; 121.3. 41.3. Calcd. For C₅₂H₄₀O₁₂ (%) C 72.89; H 4.72; O 22.41. Found: C 73.85; H 4.67; O 21.49. ESI-MS, *m/z* = 879.2 [2 + Na]⁺.

Synthesis of dodeca-benzylated pyrogallol[4]arene

Dodeca-benzylated compounds **3** and **4** were obtained via the treatment of 0.5 mmol of **1** and **2** with 4 mL of benzoyl chloride and 0.5 mL of DIPEA as a base. The reaction mixture was heated at 110 °C for 2 h. After cooling, water was added, and the mixture was extracted with chloroform. The chloroform solution was washed with a NaOH 0.1 M solution and dried with Na₂SO₄. The solvent was evaporated in a vacuum to produce a white solid (**3**) with a 40% yield and a yellow solid (**4**) with a 60% yield, which were characterized by means of IR, NMR, and ESI-MS techniques.

Dodeca-benzylated-tetra(propyl)pyrogallol[4]arene boat(rccc) (3) white solid, m.p. > 250 °C, IR(ATR/cm⁻¹): 3063 (C–H, Ar), 2957, 2871 (C–H, aliphatic), 1741 (C=O), 1441 (C=C, Ar), 1256 (C–O); RMN-¹H in CDCl₃, δ (ppm): 8.18–8.02 (m, 8H, Ar); 7.59 (m, 10H, Ar); 7.46–7.42 (m, 18H, Ar); 7.28 (m, 8H, Ar); 7.17 (m, 10H, Ar); 7.09–7.07 (m, 6H, Ar); 6.70 (s, 4H, Ar); 4.51 (s, 4H, CH); 2.05 (m, 8H, CH₂); 1.38–1.46 (m, 8H, CH₂); 0.83–0.86 (t, 12H, –CH₃). RMN-¹³C in CDCl₃ δ(ppm): 163.5; 162.2; 142.3; 139.7; 137.2; 133.4; 132.4; 131.1; 129.9; 128.3; 37.7; 37.1; 21.0; 14.1. ESI-MS *m/z* = 1993.3 [3 + Na]⁺.

Dodeca-benzylated-tetra(phenyl)pyrogallol[4]arene boat (rccc) (4) yellow solid, m.p. > 350 °C IR(ATR/cm⁻¹): 3062 (C–H, Ar), 1747 (C=O), 1440 (C=C, Ar), 1228 (C–O); RMN-¹H in CDCl₃, δ (ppm): 7.88–7.87 (m, 8H, H–Ar C=O); 7.69–7.68 (m, 6H, H–Ar); 7.56–7.54 (m, 4H, H–Ar); 7.44–7.42 (m, 6H, Ar); 7.39–7.36 (m, 12H, H–Ar); 7.24–7.19 (m, 12H, H–Ar); 7.16–7.10 (m, 24H, H–Ar); 7.06–7.02 (m, 8H, H–Ar); 6.97 (s, 2H, H–Ar); 6.76–6.73 (m, 4H, H–Ar); 6.44 (s, 2H, H–Ar); 5.77 (s, 4H, C–H). RMN-¹³C in CDCl₃, δ (ppm): 163.4; 162.5; 162.0; 141.2; 141.1; 137.0; 136.8; 133.8; 133.3; 133.1; 133.0; 132.7; 130.8; 130.2; 130.0; 129.9; 129.5; 129.0; 128.9; 128.8; 128.5; 128.4; 128.3; 128.1; 128.0; 127.9; 126.7; 126.4; 45.4. ESI-MS *m/z* = 2128.7 [4 + Na]⁺.

General procedure for the synthesis of *O*-acetylated-calix[4]pyrogallolarenes

A mixture of pyrogallol[4]arene **1** or **2** (0.4 mmol), 16 mL of acetic anhydride, and 0.3 mL of pyridine as a base was heated at 100 °C for 8 h. After cooling, 50 mL of wa-

ter was added, and the mixture was extracted with chloroform and dried with Na₂SO₄. After the removal of the chloroform, the result was a white solid with a 75% yield for compound **5** and 73% and for compound **6**, which were characterized via NMR, FT-IR, and mass spectrometry.

O-acetylated-tetra(propyl)Calix[4]pyrogallolarene (5) white solid, m.p. > 250 °C IR(ATR) ν/cm^{-1} 2936 (Ar-CH), 2872 (C-H, aliphatic), 1771 (C=O), 1370 (-C=C, Ar), 1204 (C-O); ¹H-NMR (400 MHz, DMSO-*d*₆) δ 7.17 (s, 4H, Ar), 3.95–3.99 (t, *J* 8 Hz, 4H, -CH), 2.19–2.22 (m, 20H, -CH), 1.90–1.97 (s, br, 24H, -CH₃), 1.22–1.28 (m, 8H, CH₂), 0.85–0.86 (t, *J* 4 Hz, 12H, -CH₃); ¹³C-NMR (100 MHz, DMSO-*d*₆) δ 172.3, 168.0, 167.2, 139.6, 134.8, 134.2, 123.4, 35.6, 35.5, 21.2, 20.2, 20.1, 19.9, 13.5; ESI-MS *m/z* 1247.7 [**5** + Na]⁺.

O-acetylated-tetra(phenyl)calix[4]pyrogallolarene (6) white solid, m.p. (302–304 °C); IR (ATR) ν/cm^{-1} 2937 (Ar-CH), 1778 (C=O), 1476, 1440, 1368 (-C=C, Ar), 1197 (C-O); ¹H-NMR (400 MHz, DMSO-*d*₆) δ 7.18–7.19 (m, 12H, Ar), 6.78–6.79 (m, 8H, Ar), 6.30 (s, 2H, Ar), 6.21 (s, 2H, Ar), 5.41 (s, 4H, CH), 2.17 (s, 12H, CH₃), 2.07–2.09 (m, 24H, -CH₃); ¹³C-NMR (100 MHz, DMSO-*d*₆) δ 167.1, 166.9, 166.6, 140.2, 139.4, 136.1, 136.2, 132.3, 131.9, 128.5, 128.1, 127.0, 44.0, 21.1, 19.8, 19.6; ESI-MS *m/z* = 1383.4 [**6** + Na]⁺.

NMR titrations

The ability of acylated pyrogallol[4]arene to bind with carnitine was studied in DMSO-*d*₆ via ¹H-NMR. A solution of pyrogallol[4]arene host (12 mM) was treated with various amounts of the guest carnitine (from 0.1 mM to 12 mM). After each addition, ¹H-NMR was recorded. The true guest and host concentrations in the solution were corrected for each addition. The interaction constant was determined using the changes in the chemical shift between the complex formed and host as a function of the stoichiometric host: guest ratio, and by nonlinear fitting using the Excel 365 solver tool. To indicate the formation of the complex, it is presented with the symbol @; for example, Carnitine@host.

Dynamic ¹H-NMR Experiment

A dynamic ¹H-NMR experiment was performed using a sample of crystals obtained from dodeca-acylated-pyrogallol[4]arene (**3**), and we observed a set of 1D spectra throughout the temperature range of 248 to 278 K. For NMR measurements, the pyrogallol[4]arene (**3**) concentration was 13 mM in CDCl₃. ¹H-NMR spectra at different temperatures were obtained by using a BRUKER Avance 400 (400,131 MHz, internal reference: TMS), and the chemical shifts are given in δ units (ppm). Using the coalescence temperature and the values of $\Delta\nu$ (Hz) for the ¹H-NMR spectrum for each temperature, it was also possible to establish the value of the interconversion constant using the Gutowsky–Holm equation for each temperature, and thus the Gibbs free energy (ΔG^\ddagger) values of activation could be calculated using the Eyring equation.

Spectroscopic measurements

The UV-vis absorption spectra of acylated pyrogallol[4]arenes (**3–6**) were all measured in DMSO. Stock solutions of benzylated pyrogallol[4]arenes were prepared in DMSO (1.2 mM). A stock solution of carnitine was dissolved in DMSO/H₂O 9:1 (13 mM). All the spectroscopic measurements were taken using solutions with 1.2 mM of benzylated pyrogallol[4]arenes and various concentrations of carnitine.

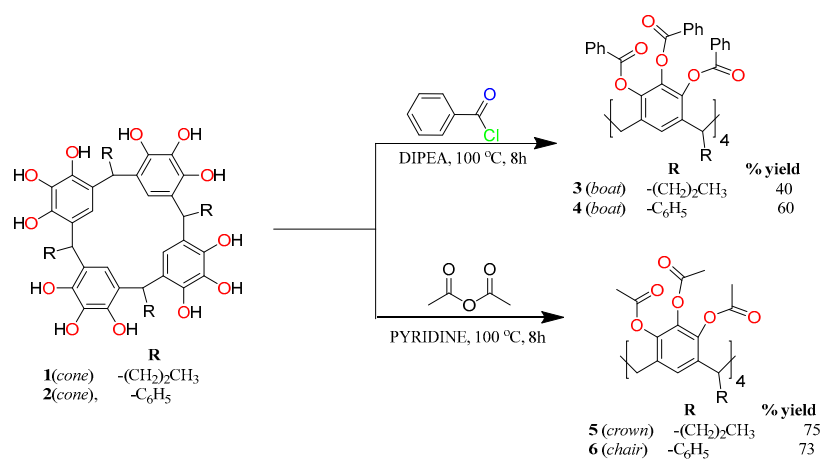
X-Ray Structure Determination

Colorless crystals of **6**·2(CH₃COOCH₂CH₃) were grown at room temperature from an ethylacetate solution by slow evaporation. The crystals were removed from the vial and covered with a layer of a viscous perfluoropolyether (FomblinY). A suitable crystal was selected with the aid of a microscope, mounted on a cryoloop, and placed in the low-temperature nitrogen stream of the diffractometer. The intensity data sets were collected at 200 K on a Bruker-Nonius KappaCCD diffractometer equipped with an Oxford Cryostream 700 unit. The molybdenum radiation used was graphite monochromated and enhanced with a MIRACOL collimator.

The structure was solved using the WINGX package [26] by direct methods (SHELXS-2013) [27] and refined by least-squares against F^2 (SHELXL-2014/7) [28]. Compound **6** crystallized with two molecules of ethylacetate, which showed disorder in atoms C(3), C(4), O(1) and O(2). This disorder was treated conventionally by using the PART tool, allowing the free refinement of the occupancy factors with the FVAR command. The final values for the occupancy factors were 61 and 39%. All non-hydrogen atoms were anisotropically refined, except those atoms of the disordered solvent molecules (atoms C(1), C(2), C(3), C(4), O(1), O(2), C(3)', C(4)', O(1)' and O(2)') that were isotropically refined. All hydrogen atoms were positioned geometrically and refined by using a riding model. Moreover, atoms C(1), C(2), O(1)' and O(2)' were restrained to lie on a plane with FLAT command [26–28].

3. Results and Discussion

For the present study, pyrogallol[4]arenes **1** and **2** were synthesized by refluxing pyrogallol and aldehyde (butyraldehyde or benzaldehyde) in ethanol in the presence of hydrochloric acid. The products were characterized using FT-IR, $^1\text{H-NMR}$, $^{13}\text{C-NMR}$, and ESI-MS techniques. These products were previously synthesized, and the spectroscopy data agree with those obtained [25]. As shown in Scheme 2, products **3** and **4** were simply prepared through a one-step reaction of **1** or **2** with benzoyl chloride in the presence of DIPEA. The formation of **3** was confirmed by the appearance of the characteristic C=O and C–O bands at 1741 and 1256 cm^{-1} , respectively. In $^1\text{H-NMR}$, the peaks at 8.18, 7.59, 7.46, 7.28, 7.17, and 7.09 ppm were assigned to new aromatic protons. The carbon signal of the carbonyl groups was observed at 163.5 ppm in the $^{13}\text{C-NMR}$ spectrum, and polybenzylation was confirmed by the molecular ion in the ESI-MS at $m/z = 1993.3$ [**3** + Na] $^+$. The characterization of **4** was performed in the same way. The FT-IR spectrum showed stretching bands at 1747 and 1228 cm^{-1} for C=O and C–O, respectively. The protons of the new aromatic bands appeared at 7.88, 7.69, 7.56, 7.44, 7.39, 7.24, and 7.16 ppm. The carbonyl signal at 163.4 ppm in the $^{13}\text{C-NMR}$ spectrum and the molecular ion in the ESI-MS at $m/z = 2128.7$ [**4** + Na] $^+$ allowed confirmation of polybenzylation. Finally, polyacetylated **5** and **6** were obtained, starting from **1** and **2** with acetic anhydride in pyridine; these derivatives were characterized using spectral techniques, including FT-IR and $^1\text{H-NMR}$. The compounds had been previously synthesized and our spectroscopic data agreed with those reported [29].



Scheme 2. Synthesis of dodeca-acetylated pyrogallol[4]arenes and dodeca-benzylated pyrogallol[4]arenes.

The *O*-acetylated tetra(phenyl)pyrogallol[4]arene **6** was also characterized by X-ray crystal structure determination. Suitable crystals were grown at room temperature from an ethylacetate solution by slow evaporation. Compound **6** crystallized with two molecules of solvent, in contrast to the previously reported solvent-free crystallographic study [30,31]. The crystallographic data for **6**·2(CH₃COOCH₂CH₃) are presented in Table 1.

Table 1. Crystallographic data for 6·2(CH₃COOCH₂CH₃).

Crystal Parameters	Data/Values
CCDC ^a deposition number	2295101
Empirical formula	C ₈₄ H ₈₀ O ₂₈
Formula weight	1537.48
Temperature	200(2) K
Wavelength	0.71073 Å
Crystal system	Monoclinic
Space group	<i>P</i> 2 ₁ / <i>n</i>
Unit cell dimensions	<i>a</i> = 11.671(1) Å <i>b</i> = 20.479(2) Å, β = 97.37(1)° <i>c</i> = 16.407(1) Å
Volume	3889.2(5) Å ³
Z	2
D _{cal}	1.313 g·cm ⁻³
Absorption coefficient	0.099 mm ⁻¹
F (000)	1616
Crystal size	0.34 × 0.28 × 0.21 mm ³
Theta range for data collection	3.03 to 27.50°
Index ranges (h, k, l)	−15 to 15, −26 to 26, −19 to 21
Reflections collected	73304
Unique data	8875 [R(int) = 0.078]
Observed data (<i>I</i> > 2(<i>I</i>))	6088
Goodness-of-fit on F ²	1.064
Final R ^b indices [<i>I</i> > 2(<i>I</i>)]	R1 = 0.072, wR2 = 0.163
R ^b indices (all data)	R1 = 0.113, wR2 = 0.190
Largest diffraction peak and hole	0.526 and −0.598 e·Å ⁻³

^a Cambridge Crystallographic Data Centre. ^b $R1 = \frac{\sum ||F_o| - |F_c||}{\sum |F_o|}$, $wR2 = \frac{[\sum w(F_o^2 - F_c^2)^2]}{[\sum w(F_o^2)^2]}^{1/2}$.

The asymmetric unit is composed of a half molecule of **6** and one molecule of ethylacetate. Figure 1 shows the complete *O*-acetylated pyrogallol[4]arene molecule, which is generated through a crystallographic inversion center. The macrocycle exhibits a *rctt* (*cis-trans-trans*) conformation, commonly known as *chair*, defined by two opposite pyrogallol rings that are not coplanar (with a separation of 0.84 Å between the planes of the rings); the two remaining pyrogallol groups inclined at 83.6° relative to the planes of the former rings.

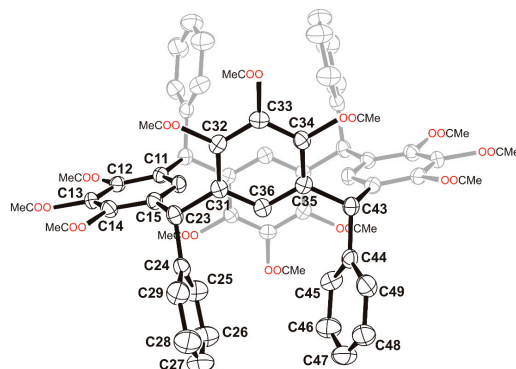


Figure 1. Perspective view of compound **6** with thermal ellipsoids at the 50% probability level. Hydrogen atoms are omitted for clarity. Symmetry code: (i) 1 − *x*, −*y*, −*z*.

Atwood et al. have proposed a set of parameters in order to accurately describe aryl-substituted pyrogallol[4]arenes and resorcin[4]arenes [31]. Firstly, the π-π distance is the separation between the centroids of the pendent phenyl groups (Figure 2, C(24)-C(29) and C(44)-C(49)), with a value of 4.520 Å. The lengths C(24)⋯C(44) and C(27)⋯C(47) are

4.872(4) and 4.165(5) Å. The difference between these C...C separations of 0.71 Å is named the tilt distance, and it expresses how much the pendent phenyl rings are tilted inwards. Finally, the angles C(27)-C(23)-C(36) and C(47)-C(43)-C(36), with values of 84.7(1) and 86.4(1)°, respectively, provide a twist angle of 8.9°, and the angle between the planes of the eclipsed pendent phenyl moieties is 34.2°. The twist angle and the angle between the planes describe the steric and torsion between the eclipsed rings. These parameters are different to those found in the previously reported solvent-free structure of **6** and other aryl-substituted *O*-acetylated pyrogallol[4]arenes [21,29], demonstrating that the positions of the pendant aryl groups are strongly influenced by crystal packing.

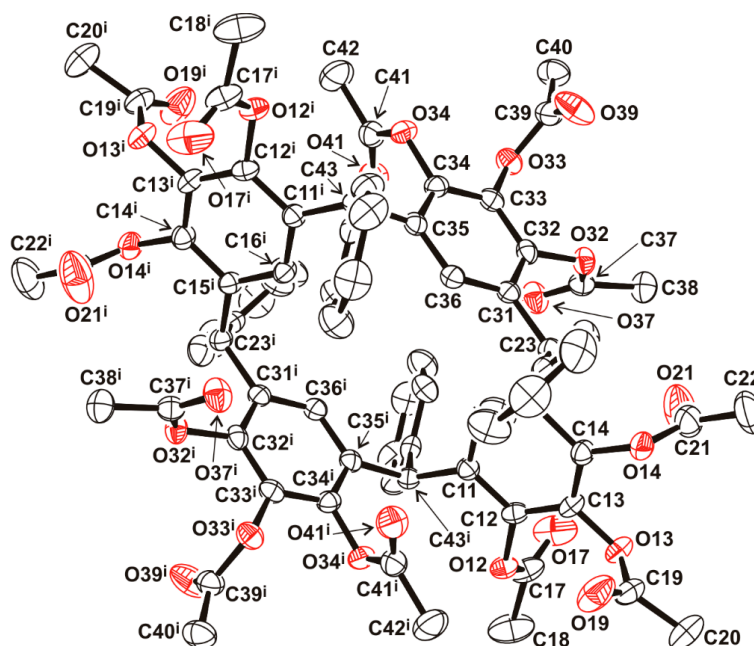


Figure 2. Simplified view of compound **6**.

Molecular interaction studies

The affinities of **1–6** with carnitine were investigated by means of NMR, mass spectrometry and UV-vis spectroscopy. First, the $^1\text{H-NMR}$ spectra of **4** at various concentrations of carnitine in $\text{DMSO-}d_6$ are shown in Figure 3. According to the spectra, the signal most affected was the methylene signal of carnitine, which split into two multiples, which indicates a strong interaction. Titration studies between **1**, **2**, **4**, **5** and **6** with carnitine were carried out, and the spectra obtained showed considerable changes, which allowed us to establish that there is an important interaction. However, the affinity of **3** for carnitine was not evidenced by any of the techniques; this behavior is analyzed later. The stoichiometric relationship was confirmed by means of electrospray ionization–mass spectrometry. The experiments were performed with different host:guest stoichiometries, producing the same signal; for example, for the 1:1 complex of carnitine with **4** (car@**4**), the signal is $m/z = 2267.1$. Table 2 shows the values obtained for the binding constants and m/z for the studied systems.

As can be seen in Figure 4, compound **4** exhibited a maximum of around 410 nm. When the macrocycle was mixed with carnitine, the color of the solution changed from orange to green, and the formed complex exhibited a maximum of around 639 nm, confirming an effective complexation. The corresponding color changed significantly from orange to green, due to the structural arrangement of pyrogallol[4]arene and the union of the cation through coordination links, which was made possible by the formation of hydrogen bonds and π -interactions in the pyrogallol[4]arene cavity. This distinct and different color change for carnitine could easily be seen by the naked eye, due to the identifiable color properties of orange and green. This benzylated tetra(phenyl)pyrogallol[4]arene-based

probe (4) potentially serves as a remarkable colorimetric probe for carnitine, with distinct color changes.

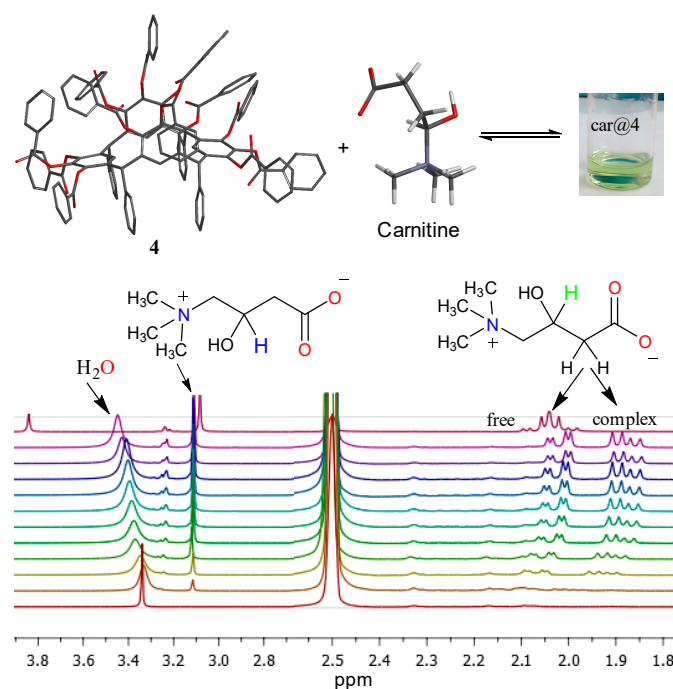


Figure 3. $^1\text{H-NMR}$ - spectra section of titration of carnitine and 4 using DMSO- d_6 as a solvent.

Table 2. Association constants between pyrogallol[4]arenes synthesized with carnitine.

Host	K_a (M^{-1}) (Carnitine@Host)	m/z
1	32.20 ± 0.14	824.6
2	36.50 ± 0.04	---
3	---	---
4	1250.20 ± 12.06	2267.1
5	12.90 ± 0.06	1385.5
6	---	1522.3

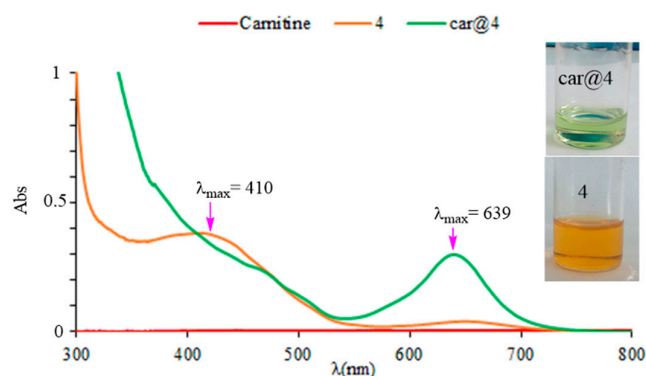


Figure 4. UV-vis spectra of 4, carnitine(car) and complex car@4 in DMSO.

Dynamic behavior of benzylated C-tetra(propyl)pyrogallol[4]arene

An explanation of the low affinity of 3 toward carnitine is the dynamic behavior of this compound in solution. As shown in Figure 5, the $^1\text{H-NMR}$ spectra of compound 3 at various temperatures were consistent with the presence of two conformers, boat A and boat B. For example, at 248 K, two resonances were observed for the methyne bridge, at

4.45 and 4.55 ppm, as well as other signals in the spectrum. This observation prompted a detailed study of the NMR spectra. It has been well established that the conformation of the pyrogallol[4]arene skeleton can be assigned in solution via a comparison of the chemical shift for the arene resonance in other analogues macrocycles, because the protons in the flattened ring are more shielded. In this way, the aromatic region exhibited two signals: one for the resonances of the aromatic protons of the pyrogallol residue on the lower rim at 6.67 ppm (hydrogen in the flattened ring) and the other at 6.71 ppm (hydrogen of the opposite aromatic ring). Other areas of the spectrum were consistent with this conformational assignment, and variable temperature effects were also observed. The temperature of coalescence was observed at 278.15 K.

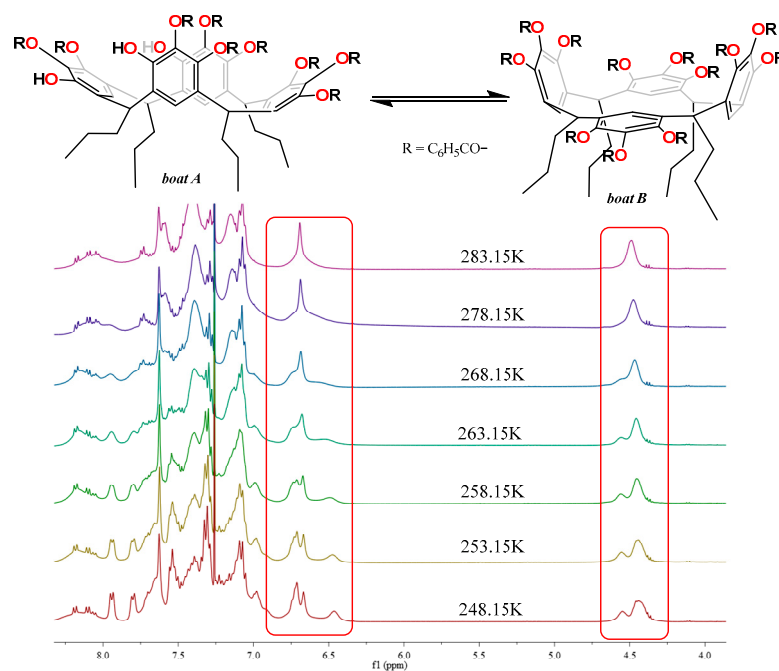


Figure 5. Dynamic NMR-1H study of **3** in CDCl₃.

The assignment of the signals for each conformer and the information of the aromatic protons in CDCl₃ at various temperatures provided data for the calculation of the conformer interconversion. Thus, the free energy of activation for the inversion (ΔG_{298}) was estimated to be 55.91 KJmol⁻¹. This value is slightly lower than that for other esters of polyhydroxylated macrocycles, which range from 60 to 65 KJmol⁻¹ [32]. In accordance with the foregoing, it is to be expected that the high molecular dynamics of **3**, involving a conformational change promoted by the few interactions at the upper rim of the macrocycle, deform the cavity; this fact constitutes a great impediment to forming the 3-carnitine complex. With compound **4**, with more bulky substituents on the lower rim, the shape of the cavity is not affected, making the process of molecular interaction with carnitine very efficient. The host-guest interaction of **5** and **6** did not present an important interaction in solution; this can be attributed to the size of the acetyl group that makes the molecule very dynamic and does not present an effective interaction with carnitine. Additionally, according to the crystallography data, **6** has a *chair* conformation; this conformation is retained in solution as previously observed, and does not favor π - π interactions.

4. Conclusions

A benzylated pyrogallol[4]arene-based colorimetric probe (**4**) was prepared by a sterification reaction with benzyl chloride. Variations in the degree of NMR spectral change were observed upon the addition of carnitine. For absorptions, different degrees of red shift, from 410 to 639 nm, were detected, and the color changes could be easily observed with the naked eye. Therefore, this benzylated tetra(phenyl)pyrogallol[4]arene-based probe could serve as

a remarkable new carnitine probe. If the polybenzylated pirogallol[4]arene has non-bulky substituents, such as the propyl group in 3, the $^1\text{H-NMR}$ spectra at various temperatures are consistent with the presence of two conformers, boat A and boat B, and the system can be dynamic for the solvent interactions. This fact impedes efficient host–guest interaction.

Supplementary Materials: The following supporting information can be downloaded at: <https://www.mdpi.com/article/10.3390/analytica5040038/s1>, Figures S1–S4: Spectroscopy information of C-tetra(propyl)pyrogallol[4]arene (crown) (1). Figures S5–S8: spectroscopic information of C-tetra(phenyl)pyrogallol[4]arene (crown) (2). Figures S9–S12: Spectroscopic information of Dodeca-benzylated-tetra(propyl)pyrogallol[4] arene boat(rccc) (3). Figures S13–S16: spectroscopic information of Dodeca-benzylated-tetra(phenyl)pyrogallol [4]arene boat (rccc) (4). Figures S17–S20: spectroscopic information of O-acetylated-tetra(propyl)Calix[4]pyrogallolarene (5). Figures S21–S24: spectroscopic information of O-acetylated-tetra(phenyl)calix[4] pyrogallolarene (6). Figure S25: $^1\text{H-NMR}$ of titration of carnitine and 1. Figure S26: $^1\text{H-NMR}$ of titration of carnitine and 2. Figure S27: $^1\text{H-NMR}$ of titration of carnitine and 4. Figure S28. $^1\text{H-NMR}$ of titration of carnitine and 5.

Author Contributions: Conceptualization, M.M., A.P.-R. and J.L.C.-H.; methodology, J.L.C.-H.; software, A.P.-R.; formal analysis, M.M., A.P.-R. and J.L.C.-H.; investigation, M.M., A.P.-R. and J.L.C.-H.; resources, M.M.; data curation, A.P.-R. and J.L.C.-H.; writing—original draft preparation, M.M., A.P.-R. and J.L.C.-H.; writing—review and editing, M.M., A.P.-R. and J.L.C.-H.; supervision, M.M.; funding acquisition, M.M. All authors have read and agreed to the published version of the manuscript.

Funding: This research received no external funding.

Data Availability Statement: The original contributions presented in this study are included in the article/Supplementary Material. Further inquiries can be directed to the corresponding author(s).

Acknowledgments: The authors would like to thank the Universidad Nacional de Colombia—Sede Bogotá and the Universidad de Alcalá de Henares, Spain.

Conflicts of Interest: The authors declare no conflicts of interest.

References

1. Flanagan, J.L.; Simmons, P.A.; Vehige, J.; Willcox, M.D.; Garrett, Q. Role of carnitine in disease. *Nutr. Metab.* **2010**, *7*, 30. [[CrossRef](#)] [[PubMed](#)]
2. Prieto, J.A.; Andrade, F.; Aldámiz-Echevarría, L.; Sanjurjo, P. Determination of free and total carnitine in plasma by an enzymatic reaction and spectrophotometric quantitation spectrophotometric determination of carnitine. *Clin. Biochem.* **2006**, *39*, 1022–1027. [[CrossRef](#)] [[PubMed](#)]
3. Minkler, P.E.; Stoll, M.S.K.; Ingalls, S.T.; Yang, S.; Kerner, J.; Hoppel, C.L. Quantification of Carnitine and Acylcarnitines in Biological Matrices by HPLC Electrospray Ionization–Mass Spectrometry. *Clin. Chem.* **2008**, *54*, 1451–1462. [[CrossRef](#)]
4. Johnson, D.W. An acid hydrolysis method for quantification of plasma free and total carnitine by flow injection tandem mass spectrometry. *Clin. Biochem.* **2010**, *43*, 1362–1367. [[CrossRef](#)]
5. Luna, C.; Griffin, C.; Miller, M.J. A clinically validated method to separate and quantify underivatized acylcarnitines and carnitine metabolic intermediates using mixed-mode chromatography with tandem mass spectrometry. *J. Chromatogr. A* **2022**, *1663*, 462749. [[CrossRef](#)] [[PubMed](#)]
6. Becker, S.; Schulz, A.; Kreyer, S.; Dreßler, J.; Richter, A.; Helmschrodt, C. Sensitive and simultaneous quantification of 16 neurotransmitters and metabolites in murine microdialysate by fast liquid chromatography-tandem mass spectrometry. *Talanta* **2023**, *253*, 123965. [[CrossRef](#)]
7. Pormsila, W.; Krähenbühl, S.; Hauser, P.C. Determination of carnitine in food and food supplements by capillary electrophoresis with contactless conductivity detection. *Electrophoresis* **2010**, *31*, 2186–2191. [[CrossRef](#)]
8. Tsiafoulis, C.G.; Exarchou, V.; Tziouva, P.P.; Bairaktari, E.; Gerothanassis, I.P.; Troganis, A.N. A new method for the determination of free L-carnitine in serum samples based on high field single quantum coherence filtering $^1\text{H-NMR}$ spectroscopy. *Anal. Bioanal. Chem.* **2011**, *399*, 2285–2294. [[CrossRef](#)]
9. Wang, M.-H.; Gu, J.-A.; Mani, V.; Wu, Y.-C.; Lin, Y.-J.; Chia, Y.-M.; Huang, S.-T. A rapid fluorescence detecting platform: Applicable to sense carnitine and chloramphenicol in food samples. *RSC Adv.* **2014**, *4*, 64112–64118. [[CrossRef](#)]
10. Andrianova, M.S.; Kuznetsov, E.V.; Grudtsov, V.P.; Kuznetsov, A.E. CMOS-compatible biosensor for L-carnitine detection. *Biosens. Bioelectron.* **2018**, *119*, 48–54. [[CrossRef](#)]
11. Mao, X.; Tian, D.; Li, H. *p*-Sulfonated calix[6]arene modified graphene as a ‘turn on’ fluorescent probe for L-carnitine in living cells. *Chem. Commun.* **2012**, *48*, 4851. [[CrossRef](#)] [[PubMed](#)]

12. Su, K.; Wu, M.; Tan, Y.; Wang, W.; Yuan, D.; Hong, M. Monomeric bowl-like pyrogallol[4]arene Ti₁₂ coordination complex. *Chem. Commun.* **2017**, *53*, 9598–9601. [[CrossRef](#)] [[PubMed](#)]
13. Ramirez, G.; Cadavid-Montoya, N.A.; Maldonado, M. Evaluation of a Resorcinarene-Based Sorbent as a Solid-Phase Extraction Material for the Enrichment of L-Carnitine from Aqueous Solutions. *Processes* **2023**, *11*, 1705. [[CrossRef](#)]
14. Castillo-Aguirre, A.; Estes, M.A.; Maldonado, M. Resorcin[4]Arenes: Generalities and Their Role in the Modification and Detection of Amino Acids. *Curr. Org. Chem.* **2020**, *24*, 2412–2425. [[CrossRef](#)]
15. Nikolelis, D.P.; Raftopoulou, G.; Psaroudakis, N.; Nikoleli, G.-P. Development of an electrochemical chemosensor for the rapid detection of zinc based on air stable lipid films with incorporated calixarene phosphoryl receptor. *Int. J. Environ. Anal. Chem.* **2009**, *89*, 211–222. [[CrossRef](#)]
16. Casas-Hinestroza, J.L.; Vela Suazo, M.Á.; Maldonado, M. Experimental comparative study of dynamic behavior in solution phase of C Tetra(phenyl) resorcin[4]arene and C-Tetra(phenyl)pyrogallol[4]arene. *Molecules* **2020**, *25*, 2275. [[CrossRef](#)] [[PubMed](#)]
17. Scott, M.P.; Sherburn, M.S. Resorcinarenes and Pyrogallolarenes. In *Comprehensive Supramolecular Chemistry II*, 2nd ed.; Elsevier: Amsterdam, The Netherlands, 2017; Volume 1, pp. 337–374.
18. Athar, M.; Das, S.; Jha, P.C.; Jha, A.M. Conformational equilibrium study of calix[4]tetrolarenes using Density Functional Theory (DFT) and Molecular Dynamics simulations. *Supramol. Chem.* **2018**, *30*, 982–993. [[CrossRef](#)]
19. Podyachev, S.N.; Syakaev, V.V.; Sudakova, S.N.; Shagidullin, R.R.; Osyanina, D.V.; Avvakumova, L.V.; Buzykin, B.I.; Latypov, S.K.; Bauer, I.; Habicher, W.D.; et al. Synthesis and properties of potassium salts of per-O-carboxymethyl calix[4]pyrogallols and their complexes with Cu²⁺, Fe³⁺, and La³⁺. *Russ. Chem. Bull.* **2009**, *58*, 80–88. [[CrossRef](#)]
20. Krause, T.; Gruner, M.; Kuckling, D.; Habicher, W.D. Novel starshaped initiators for the controlled radical polymerization based on resorcin[4]- and pyrogallol[4]arenes. *Tetrahedron. Lett.* **2004**, *45*, 9635–9639. [[CrossRef](#)]
21. Yan, C.; Chen, W.; Chen, J.; Jiang, T.; Yao, Y. Microwave irradiation assisted synthesis, alkylation reaction, and configuration analysis of aryl pyrogallol[4]arenes. *Tetrahedron* **2007**, *63*, 9614–9620. [[CrossRef](#)]
22. Jumina Setiawan, H.R.; Triono, S.; Kurniawan, Y.S.; Priastomo, Y.; Siswanta, D.; Zulkarnain, A.K.; Kumar, N. C-Arylcalix[4]pyrogallolarene Sulfonic Acid: A Novel and Efficient Organocatalyst Material for Biodiesel Production. *Bull. Chem. Soc. Jpn* **2020**, *93*, 252–259. [[CrossRef](#)]
23. Casas-Hinestroza, J.; Maldonado, M. Conformational Aspects of the O-acetylation of C-tetra(phenyl)calixpyrogallol[4]arene. *Molecules* **2018**, *23*, 1225. [[CrossRef](#)] [[PubMed](#)]
24. Maldonado, M.; Sanabria, E.; Velasquez-Silva, A.; Casas-Hinestroza, J.L.; Estes, M.A. Comparative study of the volumetric properties of three regioisomers of diazoted C-tetra(propyl)resorcin[4]arene in DMSO at various temperatures. *J. Mol. Liq.* **2021**, *325*, 115252. [[CrossRef](#)]
25. Casas-Hinestroza, J.L.; Cifuentes, A.; Ibáñez, E.; Maldonado, M. Effect of the formation of capsules of tetra(propyl)pyrogallol[4]arene on the host-guest interaction with neurotransmitters. *J. Mol. Struct.* **2020**, *1210*, 128063. [[CrossRef](#)]
26. Farrugia, L.J. WinGX and ORTEP for Windows: An Update. *J. Appl. Crystallogr.* **2012**, *45*, 849–854. [[CrossRef](#)]
27. Sheldrick, G.M. Crystal structure refinement with SHELXL. *Acta Crystallogr. Sect. C Struct. Chem.* **2015**, *71*, 3–8. [[CrossRef](#)]
28. Sheldrick, G.M. SHELXT-Integrated Space-Group and Crystal-Structure Determination. *Acta Crystallogr. Sect. A Found. Adv.* **2015**, *71*, 3–8. [[CrossRef](#)]
29. Casas-Hinestroza, J.L.; Pérez-Redondo, A.; Maldonado, M. Inclusion complexation between neurotransmitters with polyacetylated calix[4]pyrogallol arenes: ¹H-NMR and crystallographic analysis. *Res. Chem. Intermed.* **2022**, *48*, 3091–3107. [[CrossRef](#)]
30. Han, J.; Song, X.; Liu, L.; Yan, C. Synthesis, crystal structure and configuration of acetylated aryl Pyrogallol[4]arenes. *J. Incl. Phenom. Macrocycl. Chem.* **2007**, *59*, 257–263. [[CrossRef](#)]
31. Pfeiffer, C.R.; Feaster, K.A.; Dalgarno, S.J.; Atwood, J.L. Syntheses and characterization of aryl-substituted pyrogallol[4]arenes and resorcin[4]arenes. *CrystEngComm* **2015**, *18*, 222–229. [[CrossRef](#)]
32. Hoegberg, G. Two stereoisomeric macrocyclic resorcinol-acetaldehyde condensation products. *J. Org. Chem.* **1980**, *45*, 4498–4500. [[CrossRef](#)]

Disclaimer/Publisher’s Note: The statements, opinions and data contained in all publications are solely those of the individual author(s) and contributor(s) and not of MDPI and/or the editor(s). MDPI and/or the editor(s) disclaim responsibility for any injury to people or property resulting from any ideas, methods, instructions or products referred to in the content.